Effect of Non-Persistent Joint on Strength And Deformation Characteristics of Soft Rock Sample

Thesis submitted in partial fulfillment of the requirement for the degree of

Master In Engineering, Civil Engineering

by

Kingshuk Bhuin

Roll No. : 002210402021

Registration No. : 163469

Under the guidance of

Dr. Obaidur Rahaman
Assistant Professor

Department of Civil Engineering
Jadavpur University
Kolkata-700035

DECLARATION

This is to declare that I, **Kingshuk Bhuin**, student of Geotechnical Engineering Division of the Department of Civil Engineering, class roll no. **002210402021.** registation no **163469 of 2022-2023** . I have prepared this thesis entitled "**Effect of Non-Persistent Joint on Strength And Deformation Characteristics of Soft Rock Sample**" under the supervision on of Dr. Obaidur Rahaman. This manuscript is original and not directly plagiarized in any sense. However, the Literature studied for the preparation of this report has been cited wherever required and also presented in the list of references.

Kingshuk Bhuin
Roll. No.:002210402021

Registration No. :163469

Date: 14/11/2024

Department of Civil Engineering
Jadavpur University, Kolkata

CERTIFICATE

This is to certify that the thesis entitled **"Effect of Non-Persistent Joint on Strength And Deformation Characteristics of Soft Rock Sample"** has been carried out by **Kingshuk Bhuin** bearing Class Roll No: **002210402021**, and Registration No: **163469 of 2022-2023**, under our guidance and supervision and be accepted in partial fulfillment of the requirement for the degree of Master of Engineering in Soil Mechanics and Foundation Engineering in the Department of Civil Engineering.

Dr.Obaidur Rahaman
Assistant Professor
Department of Civil Engineering
Jadavpur University
Kolkata – 700032

Head of the Department
Department of Civil Engineering
Jadavpur University
Kolkata- 700032

Dean
Faculty of Engineering and Technology
Jadavpur University
Kolkata– 700032

ACKNOWLEDGMENTS

The success and completion of any project need one to walk on the right path at every step. I would like to express my profound gratitude to my guide , **Dr. Obaidur Rahaman** who gave me the golden opportunity to work on "**Effect of Non-Persistent Joint on Strength And Deformation Characteristics of Soft Rock Sample**". This seminar needed thorough study and due diligence, and he guided me thoroughly to overcome the feeble steps and to complete this project. I am truly indebted to him to work under him for this project.

I also acknowledge the cooperation and assistance provided by, Prof. Ramendu Bikas Sahu, Prof. Arghadeep Biswas, Prof. Narayan Roy and Prof. Gopinath Bhandariduring this work.

I would also like this opportunity to express my gratitude to my classmates who helped me through the entire semester with this work.

Date: 14-11-2024
Place: Kolkata

KINGSHUK BHUIN

Roll No: 002210402021
Registration No:163469
Department of Civil Engineering
JADAVPUR UNIVERSITY
KOLKATA-700035

CONTENTS

Chapter 4

Chapter 5

ABSTRACT

This study investigates the effects of displacement rates and joint orientations on the strength and deformation behavior of soft, rock-like materials, focusing on pre-existing non-persistent joints. The motivation stems from the need to understand how these factors influence material stability in geotechnical applications. Experiments were conducted on gypsum samples with intact sample and joints oriented at various angles (0˚, 15°, 30°, 45°, 60°, and 75°) and subjected to different displacement rates (1.25 mm/min, 1.5 mm/min, and 2.5 mm/min). Results reveal that higher displacement rates generally enhance the material's strength, with the effect being more pronounced in intact and favorably oriented jointed samples. The study found that samples with joints aligned parallel to the loading direction (0° and 30°) exhibited higher peak strengths than those with perpendicular orientations. Elastic modulus, stress-strain behavior, and failure patterns varied with both strain rate and joint orientation, indicating a significant influence on the material's stiffness, ductility, and fracture mechanisms. These findings provide a valuable basis for predicting the behavior of jointed rock-like materials in engineering applications where displacement rate and joint orientation are critical factors.

FIGURE INDEX

Chapter 1

INTRODUCTION

1.1 General

Rock and soil, while both foundational to geotechnical and geological engineering, exhibit distinct mechanical behaviors and structural characteristics. Unlike soil, which is generally a loose aggregation of mineral particles, rock consists of solid mineral matter with significant cohesion and strength. These differences influence how each material responds to stress, deformation, and environmental conditions. Rock's strength and stability are inherently greater than soil's, largely due to its interlocking mineral composition and more rigid structure.

However, the strength of rock is often compromised by discontinuities such as joints, faults, and fractures. These discontinuities create planes of weakness within the rock mass, affecting its ability to withstand applied loads. Unlike soil, where behavior is largely homogeneous, rock often has highly variable strength depending on the orientation, density, and connectivity of its discontinuities. The presence and characteristics of these natural planes significantly impact rock stability, influencing failure modes and reducing the material's load-bearing capacity.

Understanding these differences and the influence of discontinuities is crucial in fields like rock mechanics, where stability assessments and structural designs rely on accurate predictions of rock behavior. By studying the interaction between rock strength and discontinuities, engineers can make informed decisions about excavation, support systems, and overall project safety in rock-based environments.

1.2 Determination of Shear Strength of Rock

The shear strength of rock is a critical parameter in rock mechanics, as it directly affects stability in slopes, foundations, and underground excavations. Shear strength refers to the rock's resistance to shearing forces that act parallel to its plane. Determining this strength requires an understanding of both the intact rock material and any existing discontinuities, such as joints and fractures, as these planes of weakness can significantly reduce shear resistance.

Common laboratory methods for determining rock shear strength include the direct shear test and triaxial compression test. In the direct shear test, a rock sample is sheared along a predetermined plane, often a natural joint surface, under controlled normal and shear stress conditions. The peak and residual shear strengths are recorded to assess the rock's overall shear resistance.

The triaxial compression test provides a broader measure of rock strength, applying stress from multiple directions to simulate in-situ conditions more accurately. The shear strength can then be derived using Mohr-Coulomb criteria, which relate normal and shear stresses. For jointed rocks, the Barton-Bandis criterion is often used, which considers the roughness and strength of joint surfaces.

Field tests, such as in-situ direct shear tests and borehole shear tests**,** can also be conducted to assess shear strength under natural conditions, helping to provide more representative results for stability analyses in real-world settings. Understanding and accurately measuring shear strength is essential for reliable geotechnical designs and for predicting the behavior of rock masses under stress.

1.3 Basic Terms Related to the Mechanical Properties of Rocks:

Understanding the mechanical properties of rocks is fundamental in rock mechanics, as these properties dictate how rocks respond to stresses, deformations, and environmental conditions. Some key terms essential to rock mechanics include:

Compressive Strength: The maximum stress a rock sample can withstand under uniaxial compression. It is determined through uniaxial compressive strength (UCS) tests, where load is

applied until the rock fails, providing insights into the rock's overall strength and load-bearing capacity.

Tensile Strength: The resistance of a rock to tensile (pulling) forces, which is often much lower than its compressive strength. Tensile strength is typically measured using the Brazilian test, where a rock disc is compressed along its diameter until it fractures.
Elastic Modulus (Young's Modulus): This parameter measures the rock's stiffness, indicating its ability to deform elastically (reversibly) when subjected to stress. It is calculated as the ratio of stress to strain within the rock's elastic range, commonly determined from stress-strain curves in UCS or triaxial tests.

Poisson's Ratio: This dimensionless parameter describes the ratio of lateral strain to axial strain in a rock sample under compressive stress. It is a key factor in predicting how rocks will deform volumetrically under load.
Shear Strength: The rock's resistance to shearing forces along planes, influenced by both its intrinsic material strength and any discontinuities (e.g., joints, faults). Shear strength is often determined using direct shear tests and triaxial compression tests, applying Mohr-Coulomb or Barton-Bandis criteria.

Ductility and Brittleness: Ductility refers to a rock's ability to undergo significant deformation before fracturing, while brittleness describes its tendency to fracture without much deformation. These properties help assess a rock's behavior under different stress conditions.
These fundamental mechanical properties are essential for evaluating rock stability and behavior under various loading scenarios, supporting designs in fields such as construction, mining, and civil engineering.

1.4 Motivation:

Understanding the mechanical behavior of jointed rock formations is critical in geotechnical engineering, mining, and civil construction, where structures often rely on the stability of rock masses under varying loads. However, natural rock formations frequently contain discontinuities, such as joints and fractures, that significantly influence their strength and failure mechanisms. Among these, non-persistent joints—discontinuities that do not fully extend through the rock—pose unique challenges, as their partial nature creates complex stress distribution and strain characteristics, affecting stability in unpredictable ways.

This study is motivated by the need to simulate these conditions in a controlled laboratory setting using artificial rock samples. By creating non-persistent joints in gypsum samples and conducting Uniaxial Compressive Strength (UCS) tests, we aim to replicate and study the influence of such discontinuities on rock behavior. Additionally, investigating the effects of varying strain rates and joint orientations will provide valuable insights into the role these factors play in the deformation and failure of jointed rock masses.

The findings from this research will not only enhance our understanding of rock mechanics but also aid in developing improved predictive models for real-world applications. Ultimately, this study seeks to contribute to safer and more effective designs in fields where rock stability is a fundamental concern, such as tunnel construction, slope stabilization, and underground mining.

1.5 Objectives:

In this study, artificial rock samples will be prepared using gypsum, and Uniaxial Compressive Strength (UCS) tests will be conducted to examine their mechanical behavior. The primary objectives of the study are as follows:

i. To develop a technique for preparing rock samples with non-persistent joints**.**
ii. To investigate the stress-strain behavior of rock samples under different strain rates**.**
iii. To study the effect of joint orientation on the strength characteristics of the rock sample**.**
iv. To understand the failure mechanisms in rock samples with non-persistent joints under different strain rates and different joint orientation**.**

Through these objectives, the study aims to gain a comprehensive understanding of the mechanical properties, failure mechanisms, and behaviors of gypsum-based artificial rock samples with non-persistent joints under compressive load having various strain rates.

Chapter 2

LITERATURE REVIEW

2.1 Introduction

Rock mechanics is an integral field of study within geotechnical engineering, mining, and civil engineering, providing essential insights into the behavior of rock materials under various conditions. The examination of rock properties and their responses to different stressors is vital for ensuring the stability and safety of structures such as tunnels, slopes, and foundations. This extensive literature review encapsulates a series of pivotal studies that investigate the physical and mechanical properties of various rock types, focusing on factors such as moisture content, displacement rates, stress conditions, and sample size. These studies significantly contribute to the understanding of rock behavior, offering valuable data for practical applications in engineering and construction.

2.2 Review of Literature

In geotechnical engineering, understanding rock mechanics and the stability of rock masses under varied conditions is vital. Research has incrementally built upon this understanding by examining factors such as structural plane orientation, moisture content, loading conditions, and environmental factors. This chronological overview arranges studies by subsequent years, providing a cohesive perspective on advancements in the field.

Amadei and Goodman (1981) studied the mechanical properties of anisotropic rocks, highlighting how directional dependencies in material properties can influence rock behavior under stress. Their research focused on the impact of anisotropy—variation in material properties in different directions—on rock strength, deformability, and failure patterns. This work showed that anisotropic rocks behave differently under compressive, tensile, and shear stresses depending on the orientation of the inherent geological structures, such as layering, fractures, or foliation. These findings are critical for understanding the mechanical behavior of rocks in regions where anisotropy plays a significant role, such as in sedimentary or metamorphic rock

formations. Their work supports the findings of Zhao et al. and Hoek and Brown, underscoring the importance of anisotropy in rock mechanics studies.

Bieniawski (1984) developed the Rock Mass Rating (RMR) system, which provides a quantitative framework for assessing rock mass quality based on various geological parameters, including joint orientation, spacing, and rock strength. This rating system helps engineers classify rock masses into different categories based on their suitability for engineering projects, such as tunneling and slope construction. The RMR system incorporates factors like weathering, rock strength, and joint characteristics, offering a comprehensive tool for predicting rock mass behavior. Bieniawski's work complements the studies by Sun et al. and Gonzalez-Fernandez et al., as it emphasizes the need for detailed structural analysis and classification when assessing rock mass stability.

Atkinson (1987) examined the theoretical principles of fracture mechanics in rock failure, focusing on how cracks initiate and propagate under different stress conditions. His work laid the foundation for understanding the fracture behavior of rocks and provided critical insights into the mechanisms of crack propagation, which are central to predicting rock failure. This theoretical framework complements empirical studies on rock failure, such as those by Maji and Misra, by offering a more detailed understanding of how fractures form and propagate under applied stress, which is essential for stability analysis in rock engineering.

Goodman (1989) focused on the mechanical properties of jointed rock masses, providing a detailed analysis of how joints, fractures, and discontinuities influence the strength and stability of rock masses. His work highlighted that the mechanical behavior of jointed rocks is heavily dependent on the orientation, spacing, and persistence of joints, as well as the material properties of the rock itself. Goodman’s research emphasized the importance of considering these factors when evaluating the stability of rock masses, especially in the context of underground excavations and slope stability. His findings align with those of Sun et al. and Hoek and Brown, reinforcing the significance of structural features in rock mass behavior.

Elsworth and Bai (1992) investigated the impact of fluid flow on the mechanical properties of rock masses, particularly focusing on how changes in pore pressure and fluid saturation affect

rock strength and deformability. Their study found that the presence of fluids, such as water or oil, within rock pores can significantly alter the stress-strain behavior of rocks, leading to weakening, swelling, or other failure mechanisms. This is especially important in subsurface engineering, where fluid interactions with rock masses (e.g., in reservoirs, tunnels, or mines) can lead to unexpected stability issues. Elsworth and Bai's findings are consistent with the environmental considerations discussed by Wei et al. and Wang et al., emphasizing the need to incorporate hydrological factors into rock mechanics studies and geotechnical designs.

Palmström (1995) examined the influence of geological discontinuities, such as faults, joints, and fractures, on the mechanical behavior of rock masses. His research found that the presence of discontinuities can significantly weaken rock masses by facilitating the propagation of fractures and creating zones of weakness within the rock. Palmström's work underscores the importance of characterizing these discontinuities accurately during site investigations for geotechnical engineering projects. His findings are in line with those of Sun et al. and Zhao et al., which emphasize the critical role of joint orientation and spacing in rock mass stability.

Aydan and et al. (1996) extended their earlier work to investigate the dynamic behavior of rock masses under seismic loading conditions. They found that seismic forces can induce significant changes in the stability of jointed and fractured rock masses, with particular attention to the impact of joint orientation and spacing on seismic response. Their study provided insights into how seismic waves interact with rock masses, leading to potential failure or instability. This research is vital for the design of structures in seismically active areas, highlighting the need for dynamic analysis in seismic hazard assessments. Aydan's work supports the findings of Sun et al. and Gonzalez-Fernandez et al., reinforcing the importance of understanding dynamic loading conditions when assessing rock mass stability.

Santarelli et al. (1996) studied the mechanical response of rocks under cyclic loading conditions, where repeated loading and unloading cycles lead to progressive damage accumulation and eventual failure. Their research highlighted that rocks subjected to cyclic loading can exhibit fatigue behavior, where initial elastic deformation eventually gives way to plastic deformation and cracking. This phenomenon is important for understanding rock stability in dynamic environments, such as in earthquake-prone areas or during mining operations that

involve repeated mechanical loading. The findings complement the work of Mathur et al. and Aydan et al., emphasizing the importance of considering cyclic loading effects in the design and analysis of rock engineering projects.

Hoek and Brown (1997) developed an empirical strength criterion for rock masses that incorporates joint orientation, spacing, and weathering effects, which are crucial factors in determining the strength and stability of rock masses. Their work provides a practical framework for geotechnical engineers to assess rock mass strength, noting that joint characteristics such as persistence and orientation can significantly affect rock mass behavior. This empirical criterion has become a foundational tool in rock mechanics, supporting studies like those of Sun et al. and Gonzalez-Fernandez et al., which highlight the importance of considering structural features when evaluating rock mass stability.

Hoek (1999) focused on the design and stability of large underground excavations, providing practical guidelines for assessing the stability of caverns and tunnels in rock masses. He emphasized the importance of understanding the rock mass's behavior, including factors like joint orientation, spacing, and the overall geological setting, in ensuring the safety of large underground structures. His work introduced methods for designing tunnels and caverns with consideration of factors such as stress redistribution, excavation-induced effects, and rock mass classification. The findings from Hoek's study complement those of Sun et al. and Gonzalez-Fernandez et al., underscoring the necessity of detailed structural analysis and considering both mechanical and environmental factors in large-scale underground engineering projects.

Barla (2000) investigated the behavior of rock masses subjected to excavation-induced stresses, focusing on how rock masses respond to changes in stress conditions during tunneling and underground excavation projects. His study highlighted the critical role of rock mass strength, the presence of joints, and the interaction between excavation and in-situ stress conditions in determining stability. Barla’s research provides valuable insights into the mechanisms behind rock failure in underground environments, particularly in response to changes in stress due to excavation. His findings align with those of Wei et al. and Wang et al., underscoring the importance of understanding stress redistribution and its effects on rock mass stability during excavation.

Tabor (2000) examined the geological evolution of rock masses, specifically focusing on how tectonic processes, weathering, and other geological forces influence rock mass stability over long periods. The study demonstrated that the stability of rock masses can change over geological timescales, particularly in tectonically active regions. This research provided insights into the long-term behavior of rock masses, including how deformation and fracturing can evolve under different geological conditions. Tabor's work emphasized the importance of considering the historical and evolving nature of rock mass stability in geotechnical engineering projects. This aligns with the research by Sun et al. and Aydan et al., highlighting the need to consider geological history in stability assessments.

The Itasca Consulting Group (2002) developed FLAC, a numerical modeling software designed to simulate the behavior of rock masses under various loading conditions. FLAC uses the finite difference method to model the deformation, stress, and failure mechanisms in rock and soil, making it a powerful tool for geotechnical engineering projects. Their work emphasizes the importance of using numerical simulations to understand complex interactions between rock properties, environmental factors, and loading conditions. FLAC has become a widely used tool for rock mechanics and stability analysis, complementing the empirical studies by Sun et al. and Gonzalez-Fernandez et al., providing a computational framework for assessing the stability of rock masses.

Potyondy and Cundall (2004) developed the Particle Flow Code (PFC), a numerical method for simulating the behavior of granular and jointed rock masses under various loading conditions. The PFC method models the interaction between particles or blocks, allowing for a more accurate representation of rock mass behavior, especially in cases involving discontinuities or complex loading patterns. Their work expanded the capabilities of discrete element modeling (DEM) to simulate more realistic fracture patterns and failure mechanisms in rock masses. This approach complements the FLAC software developed by the Itasca Consulting Group, providing another powerful tool for numerical simulations of rock mass behavior, particularly for problems involving granular media or highly fractured rocks.

Lato et al. (2012) explored the use of terrestrial laser scanning (TLS) for monitoring rock slope stability. They demonstrated that TLS can capture high-resolution 3D data of rock slopes,

allowing for accurate monitoring of deformation and potential failure zones. The study highlighted the importance of these advanced remote sensing technologies for improving early warning systems and providing more precise data on rock mass stability over time. The findings of Lato et al. align with the studies by Chen et al. (2017) on LiDAR and InSAR technologies, emphasizing the role of advanced surveying and monitoring methods in geotechnical engineering for managing rock mass stability.

De Jong et al. (2013) explored the role of bio-geotechnical processes, such as microbial-induced calcite precipitation (MICP), in improving the strength and stability of rock masses. Their research demonstrated that certain microorganisms could facilitate the precipitation of minerals within rock pores, effectively improving the cohesion and mechanical properties of weak or fractured rocks. These bio-geotechnical approaches represent an innovative solution for stabilizing rock masses in environmentally sensitive areas or for sustainable geotechnical practices. This aligns with the environmental considerations discussed by Wei et al. and Zhang et al., offering new avenues for geotechnical engineers to improve rock mass stability using natural processes.

Zhao and et al. (2016) focused on the mechanical behavior of anisotropic rocks, emphasizing that directional dependencies in rock properties significantly influence their stability and strength under various loading conditions. Their findings suggest that the mechanical properties of anisotropic rocks, such as strength and deformability, are highly sensitive to the direction of applied stress. The study highlights the importance of incorporating directional dependencies when analyzing the stability of rock masses, supporting earlier research by Sun et al. and Gonzalez-Fernandez et al. on the role of structural characteristics in rock mass behavior.

Jones et al. (2016) explored the impact of tectonic stress fields on the stability of rock masses, combining geological mapping, seismic data, and mechanical testing to develop a comprehensive model of tectonic influences. Their research showed that tectonic stresses can significantly alter the mechanical properties of rocks, leading to localized failure or mass instability. This integrative approach highlights the importance of considering tectonic stress in rock mass stability assessments, supporting the findings of Sun et al. and Aydan et al., which stress the need for detailed geological and geophysical data in stability analyses.

Kwasniewski et al. (2017) examined the impact of underground mining on rock mass stability, showing that mining-induced stresses can lead to significant alterations in the mechanical properties of the surrounding rock. The researchers found that excavation activities, especially in deep mines, can induce fractures and cause rock mass weakening, leading to potential collapse or failure. This study emphasizes the need for careful planning and monitoring of mining operations to prevent catastrophic failures. Their findings align with Barla's work on excavation-induced stresses and Palmström's research on geological discontinuities.

Chen et al. (2017) explored the application of LiDAR (Light Detection and Ranging) and InSAR (Interferometric Synthetic Aperture Radar) technologies for monitoring the stability of rock slopes. These remote sensing techniques allow for high-resolution monitoring of slope deformation over time, enabling early detection of potential failure zones. Their findings demonstrate the effectiveness of these technologies in providing detailed, real-time data on rock mass behavior, which can be critical for mitigating risks in geotechnical engineering projects. This research supports the findings of Sun et al. and Gonzalez-Fernandez et al., offering new tools for assessing and managing stability risks in rock masses.

Maji and Misra (2018) analyzed the influence of displacement rate and joint persistence ratio on fracture patterns in rocks, showing that both factors significantly impact rock failure. As displacement rates increase, rock strength improves up to a critical point, after which the strength declines as fractures develop. Additionally, the persistence of joints, or the continuity of fractures in the rock, influences fracture propagation, with non-persistent joints leading to more complex fracture patterns. Their study provides insights into how joint characteristics and displacement rates must be carefully considered in rock engineering to predict failure and design more stable structures.

Singh et al. (2018) investigated the mechanical interaction between sandstone and shale layers in sedimentary basins, revealing that the presence of weaker shale layers can significantly influence the overall stability of the rock mass. Their study demonstrated that the mechanical behavior of layered rock masses is complex, with the strength of the weaker shale layers playing a pivotal role in the stability of the entire structure. This research supports the findings of Sun et al. and

Zhao et al., underscoring the importance of understanding the interactions between different types of geological formations when assessing rock mass stability.

Wang et al. (2018) investigated the effects of water-rock interactions on rock strength degradation, finding that prolonged water exposure weakens rock masses, reducing their strength and durability. Their study emphasizes the potential risks associated with water infiltration in underground constructions like tunnels, where water can significantly destabilize rock masses over time. The researchers' findings underscore the importance of considering water-rock interactions in the design of structures that interact with moist environments, as they can lead to significant long-term weakening and failure of rock materials.

Li et al. (2018) researched the use of fiber optic sensors for monitoring strain, temperature, and other critical parameters in rock masses. The study showed that fiber optic sensors offer high precision and durability in underground environments, providing real-time data on the behavior of rock masses under various conditions. This technology is particularly beneficial for monitoring rock slopes, tunnels, and other geotechnical structures where continuous data on stability is crucial. Li et al.'s work complements the empirical and numerical methods described by Hoek and Brown and the Itasca Consulting Group, offering new capabilities for real-time monitoring and more informed decision-making in geotechnical projects.

Zhang et al. (2019) explored the thermal effects on the mechanical properties of rocks, revealing that exposure to high temperatures can significantly reduce rock strength and alter failure modes. Their research showed that rocks exposed to elevated temperatures exhibit decreased strength and transition to more ductile failure behavior, similar to the plastic failure seen in gypsum-like materials under moisture loss. The study highlights the need to account for thermal conditions in geotechnical engineering, especially in environments where high temperatures could affect the stability and integrity of rock masses, such as in mining or tunnel engineering.

Wei et al. (2019) examined the role of moisture content in the physical and mechanical properties of gypsum-like rocks, finding that water saturation increases the density and wave velocity of gypsum samples, enhancing their stiffness. Dehydration at high temperatures, however, induces plastic failure behavior, shifting the rock’s failure characteristics from brittle to

ductile. This finding has important practical implications, particularly for tunnel construction in gypsum-rich regions, where water exposure could lead to rock expansion and stability issues. The study underscores the need to consider moisture content in geotechnical projects involving gypsum-like materials.

Smith et al. (2019) explored the impact of mineralogical composition on the mechanical properties of shale, demonstrating that variations in mineral content can significantly affect rock strength and deformability. Their study found that the presence of certain minerals, such as clay minerals, can weaken rock, while others, like quartz, enhance its strength. This research is particularly relevant for the study of rocks like shale, which often contain varying mineral compositions that can influence their behavior under stress. Smith et al.'s work complements the findings of Gonzalez-Fernandez et al. and Mathur et al., highlighting the importance of considering material composition in rock mechanics studies.

Gaurav Kumar Mathur et al (2020) studied the effect of displacement rates on the mechanical properties of soft-porous rock analogs containing non-persistent joints. The researchers found that rock strength increases with displacement rates up to a critical threshold, beyond which strength begins to decrease as damage accumulates. This critical displacement rate is associated with the onset of fracture propagation, which weakens the material. The findings highlight the importance of considering displacement rates when evaluating the mechanical behavior of jointed rock masses and suggest that beyond a certain rate, rocks may exhibit weaker behavior due to micro-crack initiation and propagation.

Shaorui Sun et al. (2020) explored the impact of structural planes in rock masses on the stability of slopes, particularly focusing on the spillway lock chamber slope of the Liyuan hydroelectric station. Their study found that the orientation of structural planes—especially those with dip angles between 45° and 60°—significantly influences slope stability. Additionally, the number of structural planes and their spacing also affected rock mass stability. The researchers employed triaxial testing on rock samples, confirming that the alignment, spacing, and number of structural planes must be carefully considered when assessing the stability of rock slopes in engineering projects.

Li et al. (2020) examined the long-term effects of freeze-thaw cycles on rock mass stability, particularly in cold regions. Their research found that repeated freeze-thaw cycles lead to significant degradation of rock strength, as the expansion and contraction of water within rock pores can cause microfracturing and weakening of rock masses. This phenomenon is particularly concerning for engineering projects in regions subject to freeze-thaw conditions, such as tunnels and foundations in mountainous or polar areas. The study highlights the need to consider freeze-thaw cycles in geotechnical designs, particularly in light of changing climate patterns that may exacerbate this effect. Their findings align with those of Wei et al. and Zhang et al., emphasizing the role of environmental factors in rock mass stability

Zhang et al. (2020) studied the influence of heterogeneity in rock masses on their mechanical properties and fracture patterns. The research found that variations in material properties, such as differences in mineral content, porosity, or grain size, can lead to significant differences in how rocks respond to stress and deform. Heterogeneity can create zones of weakness that affect the propagation of fractures and the overall strength of the rock mass. This study is particularly relevant to the work of Gonzalez-Fernandez et al. and Mathur et al., as it emphasizes the importance of considering material heterogeneity in both laboratory and field studies to accurately predict rock mass behavior.

Manuel A. Gonzalez-Fernandez et al. (2021) investigated the size-dependent behavior of Blanco Mera granite under triaxial loading conditions, revealing that the strength of the rock decreases with increasing sample size, particularly under low confining pressures. Larger rock samples exhibit more brittle behavior than smaller ones, especially at lower confinement, due to micro-crack closure at higher confining pressures. This research emphasizes the need to account for both sample size and confining pressure when testing rock strength, as larger samples tend to behave differently compared to smaller ones in terms of failure mode and mechanical properties.

Huang et al. (2021) investigated the potential of machine learning algorithms in predicting rock mass behavior under various conditions. By analyzing large datasets of rock properties, environmental factors, and loading conditions, their models were able to accurately predict rock failure patterns and mechanical responses. This approach represents an innovative leap in geotechnical engineering, enabling more efficient and accurate predictions of rock mass

behavior. Their work aligns with the empirical and numerical methods discussed by Hoek and Brown and the Itasca Consulting Group, providing a modern, data-driven tool for enhancing rock mechanics analysis.

2.3 Summary

The reviewed studies collectively advance the understanding of rock mechanics, emphasizing the significance of factors such as displacement rates, stress conditions, jointing, and sample size on the mechanical properties of various rock types. These insights are crucial for geotechnical engineering, mining, and civil engineering applications, where the stability and safety of rock structures are paramount. By considering these factors, engineers and researchers can better predict rock behavior under different conditions, leading to more effective and reliable design and construction practices. The detailed analyses and findings from these studies provide a robust foundation for future research and development in rock mechanics, contributing to the ongoing efforts to enhance the safety and efficiency of engineering projects involving rock materials. Through continuous exploration and understanding of these dynamics, the field of rock mechanics will continue to evolve, offering innovative solutions to complex geological challenges and ensuring the stability and durability of vital infrastructure projects. The study of the effects of non-persistent joints on rock behavior remains relatively underexplored. Therefore, this thesis aims to address this gap by conducting a detailed investigation into how these joints influence the mechanical properties and failure characteristics of soft rock analogs.

Chapter 3

METHODOLOGY

3.1 Introduction

Experimental studies on jointed rocks are essential for understanding the mechanical behavior of rock masses and their responses to stress. These studies generally fall into two categories: those utilizing natural rock formations with existing joints or creating artificial joints using machinery, and those using synthetic materials to simulate rock behavior under controlled conditions. Each approach has its own set of advantages and limitations.

3.2 Preparation of Samples

The samples were prepared using plaster of paris ($CaSO4 \cdot 1/2H2O$), which was mixed with water in a 1:0.5 weight ratio to form gypsum ($CaSO4 \cdot 2H2O$). This mixing ratio ensures that the gypsum mixture achieves the desired consistency and strength.

The Polyvinyl chloride (PVC) pipes, measuring 100mm and 50mm in diameter, were cut to create the molds. The horizontal and vertical axis were carefully determined and marked for accuracy. Desired angles were then indicated on the pipes, and using a hacksaw, the pipes were cut to form the molds with the specified angles.

The mixture was subsequently poured into cylindrical PVC molds with a diameter of 50 mm and a height of 100 mm. A consistent range of vibration was applied to ensure uniform density across all samples. To achieve a smooth bottom surface, a rubber sheet was securely attached to the bottom of the mold. Additionally, a smooth knife was used to level and refine the top surface.

Then the samples were left to air-dry at room temperature for approximately 10 days, allowing sufficient time to achieve the necessary cohesion and strength in the gypsum. Initially, each sample's weight was recorded immediately after casting. A second weight measurement was taken after the air-drying period to confirm that all specimens had reached identical mass. This process ensured uniformity in both mass and density across all individual specimens.

Fig 3.1: PVC moulds with cracks having orientation such as 0˚, 15˚, 30˚, 45˚, 60˚, 75˚ for the preparation of rock sample.

3.3 Experimental Setup and Sample Configuration

To ensure reproducibility and consistency in the experiments, close attention was given to the mixing, casting, and processing steps. Two distinct sets of samples were prepared for testing

Intact Samples: These samples were prepared without joint segments and served as a baseline for comparison with the jointed samples.

Single Joint-Segmented Samples: For these samples, a single joint segment was introduced at varying angles relative to the cylinder axis. The tested angles included 0°, 15°, 30°, 45°, 60°, and 75°.

To create the joint segments, a thin, planar aluminum slit with a thickness of 0.15 mm was inserted into the gypsum sample at each predetermined angle.

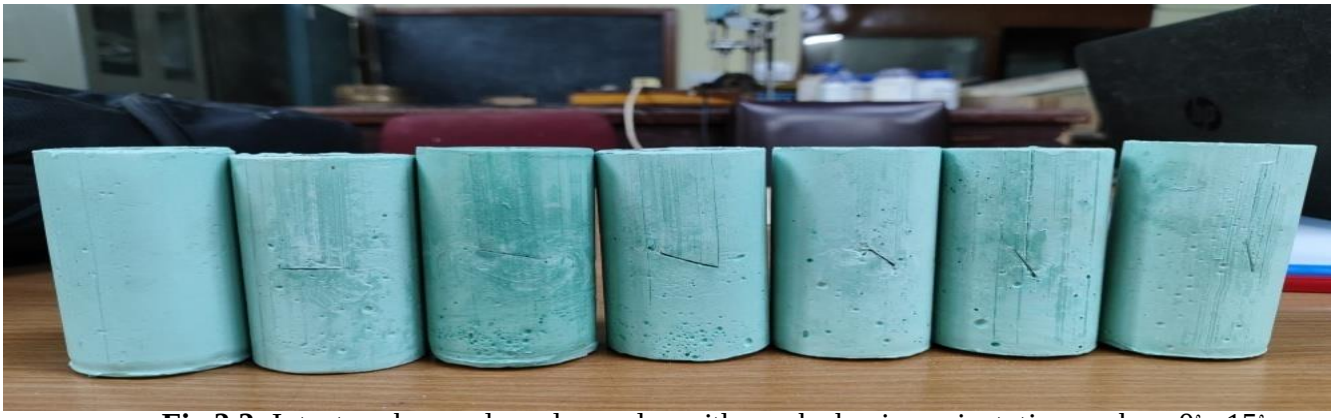

Fig 3.2: Intact rock sample and samples with cracks having orientation such as 0˚ , 15˚, 30˚, 45˚, 60˚, 75˚

3.4 Experimental procedure:

Compression tests were conducted using a uniaxial testing machine set to displacement-controlled mode, selected for its suitability to the experimental requirements. With a maximum load capacity of 50 kN, the machine was well-suited to handle the anticipated strength and deformation characteristics of the samples.

Three uniaxial displacement rates—1.25 mm/min, 1.5 mm/min, and 2.5 mm/min, were applied during testing. The datasheet was prepared by recording the proving ring readings at intervals corresponding to every 20 divisions on the dial gauge, ensuring consistent data collection across each sample.

Data from the proving ring is recorded at consistent intervals (every 20 divisions on the dial gauge), which ensures uniformity in the data collection process and enables direct comparisons across samples with intact and jointed configurations.

Stress is determined by dividing the measured load (from the proving ring) by the cross-sectional area of the sample. This calculation provides a stress value corresponding to each load measurement.

Strain is calculated by dividing the displacement values by the original length of the sample. These strain values are aligned with the corresponding load data to track the material's deformation over the course of the test.

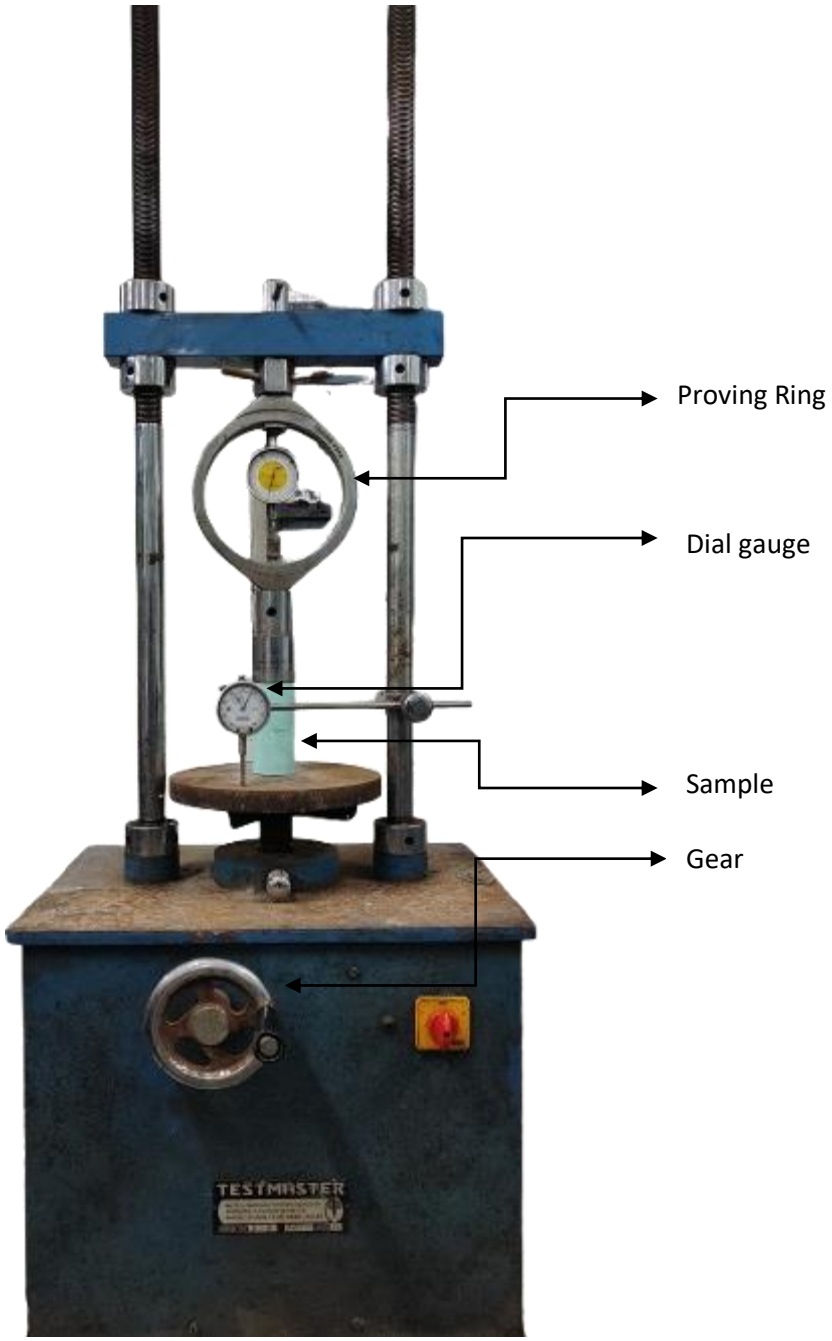

Fig 3.3 Unconfined compression testing machine

Chapter 4

RESULTS & DISCUSSIONS

4.1. Stress-Strain Behavior:

Investigating the stress-strain response of gypsum under compressive loading provides valuable insights into its structural behavior and mechanical properties, which are crucial for applications requiring stability and durability. Gypsum, widely utilized in construction and engineering contexts, demonstrates specific characteristics when subjected to compressive forces, shedding light on its elasticity, strength, and failure mechanisms. This study involved conducting uniaxial compression tests on gypsum samples, both in intact form and with a single joint segment at various angles. By introducing a joint at predetermined angles, the study explored how these segments influence gypsum's ability to withstand and deform under stress. Different displacement rates (1.25 mm/min, 1.5 mm/min, and 2.5 mm/min) were applied using a uniaxial testing machine, generating data for calculating and plotting stress-strain curves for each sample type. These curves provide a detailed view of key properties, such as modulus of elasticity, peak stress, and strain at failure. The findings from this testing offer a clearer understanding of gypsum's behavior under compressive forces, particularly in relation to joint orientation and displacement rate. This information is valuable for applications that depend on gypsum's load-bearing capacity and stability, informing material selection and engineering practices in design and construction field.

A. Intact Sample:

For intact sample Fig 4.1 the stress-strain curve begin with a linear region where stress increases proportionally with strain. This initial phase represents the elastic behavior of the material. The slopes of these initial linear portions appear similar across the different strain rates, indicating a consistent elastic modulus (stiffness) regardless of strain rate. After the initial linear region, each curve reaches a peak stress point, which can be associated with the yield strength of the material. The peak stress varies depending on the strain rate, for intact sample of strain rate of 2.5mm/min Fig 4.1 stress strain curve has the highest peak stress, reaching about 9.5 N/mm^2 . For the strain rate of 1.5 mm/min the peak stress is slightly lower, reaching around 8 N/mm^2. And for strain rate of 1.25 mm/min this has the lowest peak stress, peaking around 7 N/mm^2. Higher strain rates result in higher peak stresses, indicating that the material can withstand higher stresses before yielding when subjected to a faster strain rate. For 2.5 mm/min, peak stress occurs around a strain of 0.02. For 1.5 mm/min strain rate, the peak stress occurs at a slightly lower strain of about 0.018. For 1.25 mm/min strain rate, the peak occurs at approximately 0.016 strain. This trend shows that higher strain rates result in a greater strain at the peak stress. After reaching the peak stress, each curve shows a decline, indicating material softening and eventual failure. The rate of decline varies are observe as, for 2.5 mm/min strain rate the curve has a slower decline, maintaining higher stress values over a larger strain range before tapering off, which suggests that the material has a better ability to sustain stress under high strain rates. For strain rate of 1.5 mm/min, the decline is steeper than the 2.5 mm/min curve, indicating quicker stress reduction after peak.1.25 mm/min, The steepest decline, showing rapid loss of stress-bearing capacity post-yield, which implies a more brittle failure characteristic at this lower strain rate.

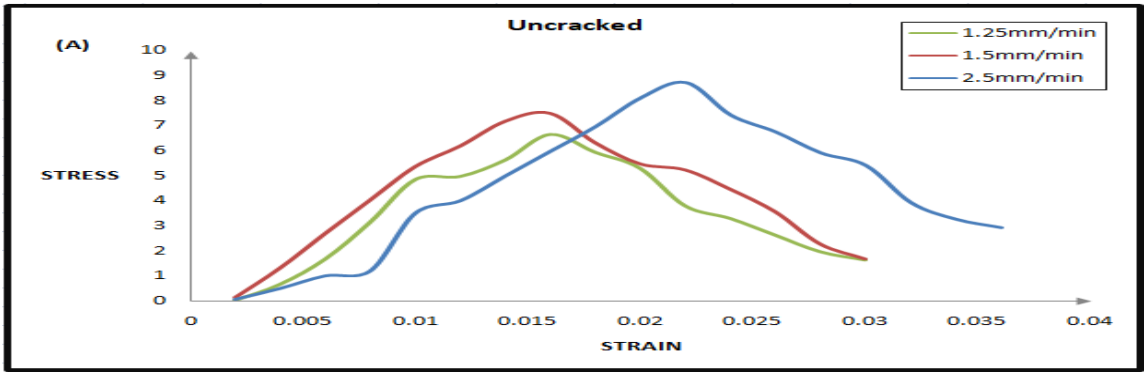

Fig 4.1: Stress-strain curve of intact sample under different strain rates

B. Non-persistent joint Sample:

The stress-strain behavior of samples with non-persistent joint at various angles and tested under different strain rates of 2.5 mm/min, 1.5 mm/min, and 1.25 mm/min. In general, strain rate influences the material's ability to withstand stress before failure. As we observe across the Fig 4.2. for strain rate of 2.5 mm/min, the peak stress values reach around 8-9 N/mm^2 for certain crack orientations, indicating the material's higher capacity to resist stress under rapid loading conditions. The stress-strain curves for different crack angles display prominent peaks before declining, suggesting a brittle or sudden failure mode at high strain rates. The high peak stresses observed could be due to the material's limited time to deform and dissipate energy, resulting in greater resistance to crack propagation and fracture. For strain rate of 1.5 mm/min, the maximum stress values are lower, generally in the range of 6-7 N/mm^2. This reduction in peak stress suggests that as the strain rate decreases, the material has more time to undergo plastic deformation or to experience internal structural changes that reduce its capacity to bear high stresses. This strain rate still shows distinct peak stresses based on crack orientation, but the material's resistance to stress is evidently lower than at 2.5 mm/min. For strain rate of 1.25 mm/min, the results in peak stresses mostly below 6 units, with the stress-strain curves appearing more flattened and less sharply peaked than at the higher strain rates. This pattern indicates a more ductile behavior, where the material can accommodate more deformation at lower stress levels. The gradual nature of the stress decline also suggests that, under slow loading, the material has sufficient time for crack propagation and plastic deformation, leading to an extended failure process rather than a sudden one.

There are samples with cracks of six different angles such as 0°, 15°, 30°, 45°, 60°, and 75°. Crack orientation strongly influences the maximum stress the material can withstand before failure. 0° and 30° crack orientations sample yield the highest peak stresses across all strain rates, indicating greater resistance to failure. Cracks aligned closer to the load direction (0°) or slightly offset (30°) are better able to bear higher loads before stress reaches critical levels. This could be due to the load path being better aligned with the crack direction, allowing the material on either side of the crack to share the load more effectively, delaying crack propagation. 15° and 45° crack orientations show intermediate peak stress levels. For example, at the 1.5 mm/min strain rate, the 45° crack angle achieves a moderate peak, lower than 0° but still higher than 75°. The

orientations allow partial alignment of the load with the crack, enabling moderate load transfer and stress resistance. However, they are not as effective as 0° or 30° orientations in distributing load, which reduces their peak stress capacity. 60° and 75° crack angles sample consistently exhibit the lowest peak stresses across all strain rates. When the crack orientation is closer to being perpendicular to the load direction, the material is more susceptible to crack opening and propagation, which rapidly reduces its load-bearing capacity. In this orientation, the crack acts as a weak point under load, easily facilitating fracture, and leading to early failure. At higher strain rates, the stress peaks for these orientations are still noticeably lower than for lower-angled cracks, highlighting their vulnerability. For strain rate of 2.5 mm/min the stress-strain curves show distinct, high peaks for each crack angle. Differences between angles are clearly defined, with 0° and 30° cracks reaching the highest peaks and 60° and 75° angles showing lower peaks. This indicates that, under high strain rates, crack orientation has a pronounced effect on stress tolerance, likely because the material has minimal time for plastic deformation, making crack propagation behavior more angle-dependent. At 1.5 mm/min strain rate the peak stresses are reduced compared to 2.5 mm/min, and while the differences between crack angles are still visible, they are less pronounced. The stress-strain curves display slightly smoother peaks, suggesting that the material can undergo limited plastic deformation before failure. Here, the impact of crack angle remains evident, with lower angles still bearing more load than higher angles, but overall resistance to stress is diminished compared to the higher strain rate. At 1.25 mm/min strain rate the stress peaks are lower and appear more spread out for each crack angle, suggesting a more gradual failure mechanism. The curves for different angles are closer together, indicating that, at low strain rates, the effect of crack orientation is somewhat diminished. This strain rate allows more time for crack growth and deformation, resulting in lower peak stresses across all orientations. The gradual decline in stress following the peak suggests the material is able to deform more before failure, which is consistent with ductile behavior.

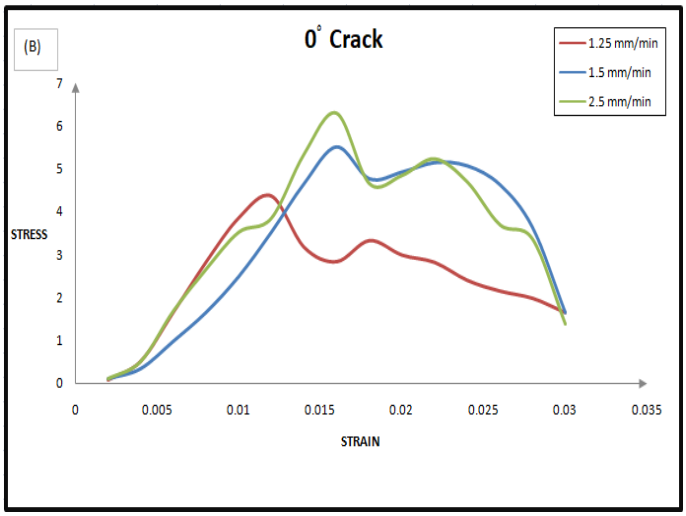

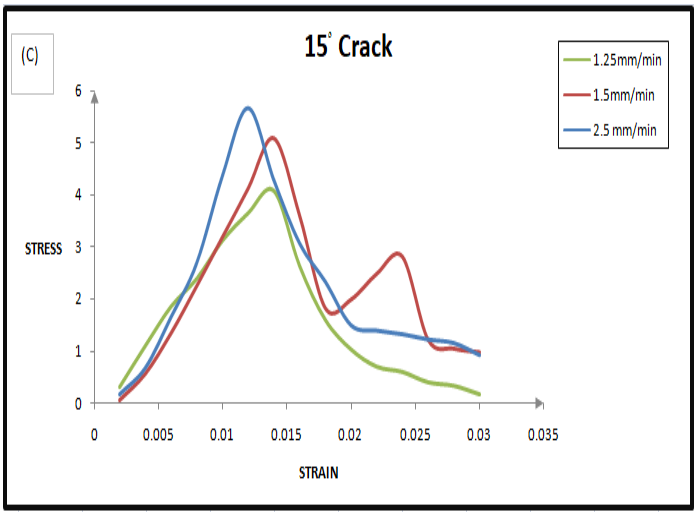

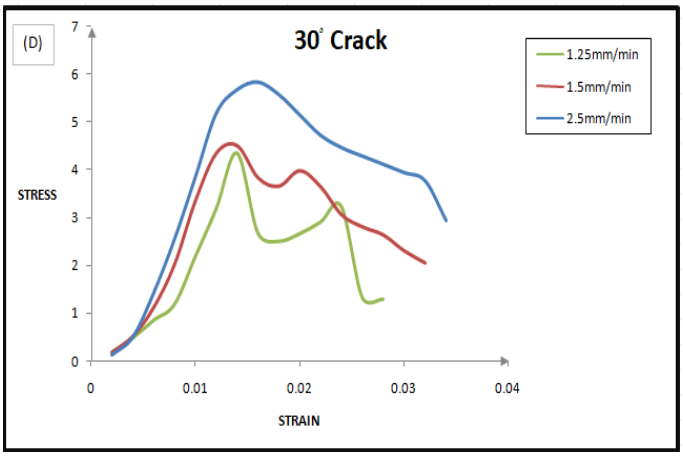

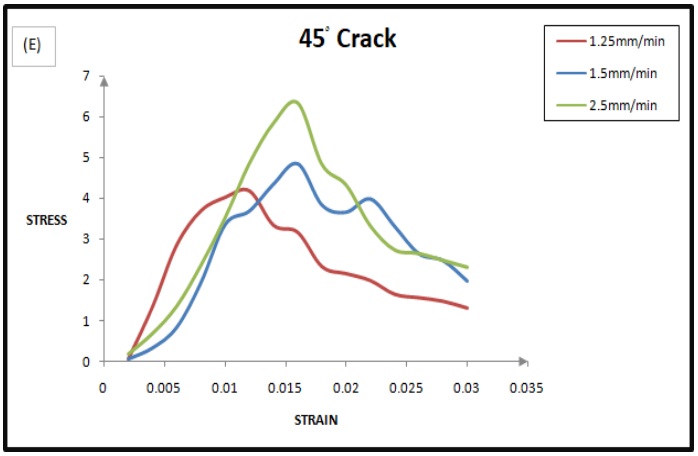

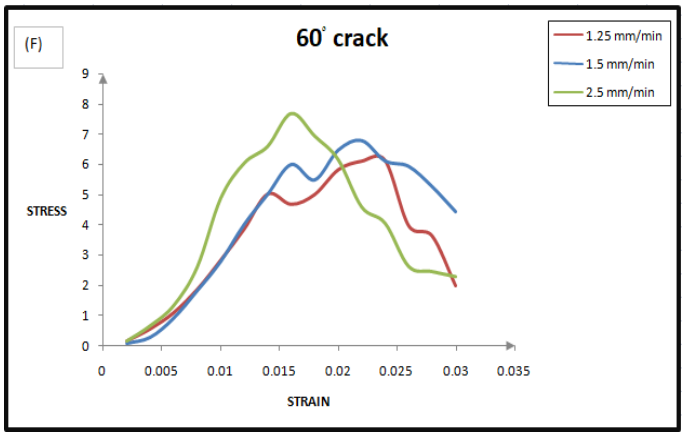

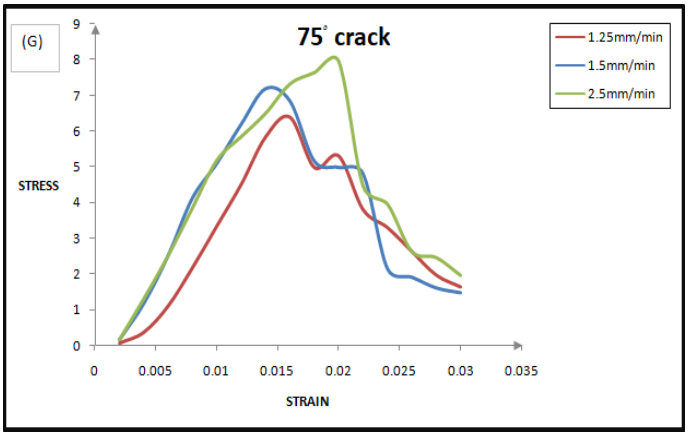

Fig 4.2 Stress-strain curve for different strain rate
(B)0˚ crack sample, (C)15˚ crack sample,(D)30˚ crack sample,(E)45˚ crack sample,
(F)60˚ crack sample, (G)75˚ crack sample

4.2 Variation of Elastic modulus:

The variation in the elastic modulus for gypsum samples with different crack angles and three loading rates (2.5 mm/min, 1.5 mm/min, and 1.15 mm/min). The elastic modulus values change according to both the crack angle and the loading rate, revealing important trends in the material's stiffness under these conditions. The data table includes three different loading rates, each influencing the elastic modulus of gypsum samples with various crack angles: For higher loading rate, 2.5mm/min generally, higher modulus values are observed for most angles. Moderate loading rate 1.5mm/min modulus values tend to be slightly lower than 2.5 mm/min, but still follow similar trends. For lower loading rate 1.25mm/min the modulus values decrease more significantly for specific crack angles, especially at lower angles.

A. Elastic Modulus for the Intact (Uncracked) Sample

The intact sample serves as the baseline for stiffness comparison across different crack angles, for each loading rate, the intact sample shows relatively high elastic modulus values. Elastic modulus decreases as the loading rate decreases, indicating that the intact sample becomes slightly less stiff with slower loading rates. This is typical in materials where strain rate can impact measured stiffness.

B. Effect of Crack Angle on Elastic Modulus at Different Loading Rates

The 0° crack angle with 2.5mm/min strain rate the elastic modulus is 445.995 N/mm^2, slightly lower than the intact sample, indicating a modest reduction in stiffness. For 15° to 60° crack angles with 2.5mm/min strain rate, the elastic modulus increases at these intermediate crack angles, with the highest value of 588.078 N/mm^2 observed at 60°. This suggests that at higher loading rates, certain crack orientations might "lock" or resist deformation better than others, resulting in higher stiffness. For 75° crack angle the elastic modulus returns closer to the intact sample's value, with a slight reduction at 445.898 N/mm^2, suggesting minimal impact at this angle.

The 0° crack angle with 1.5mm/min strain rate the modulus drops more significantly to 403.278 N/mm^2, showing a larger reduction in stiffness as compared to the intact sample as 551.714 N/mm^2. This is likely due to the alignment of the crack with the loading direction, which opens up more readily under slower loading. Again for 15° to 60° crack angles the elastic modulus

increases at 15° and 30° but then decreases at 45° and 60°, following a non-linear trend. The modulus value at 15° is relatively high as 427.647 N/mm^2, and then it decreases with higher angles, with a notable drop at 45° as 376.851 N/mm^2. And for 75° crack angle the modulus slightly increases again to 402.214 N/mm^2, approaching the intact value at this loading rate, showing that near-perpendicular cracks have less impact on stiffness.

The 0° crack angle with 1.25mm/min strain rate the elastic modulus shows the most substantial drop at 205.029 N/mm^2, indicating a major reduction in stiffness. This large reduction aligns with the tendency of rock sample to exhibit weaker behavior under slow loading rates when cracks are aligned with the loading direction. 15° to 45° Crack Angles: There is a gradual increase in modulus as the crack angle increases, reaching 420.463 N/mm^2 at 45°. The cracks are oriented obliquely, which helps resist deformation slightly better under slower loading conditions. 60° and 75° Crack Angles: Modulus values are slightly lower than the intact sample but still remain high compared to lower angles, with 410.315 N/mm^2 and 494.465 N/mm^2, respectively. The 75° angle even surpasses the modulus of the intact sample, which could indicate that cracks at steep angles have a minimal effect on stiffness at very low loading, cracks open more readily, leading to higher deformability and reduced stiffness. Angles around 15° to 45° show varying effects on the modulus, with some increasing stiffness at higher loading rates (suggesting possible crack "closure" under fast loading) and others reducing stiffness at slower rates due to increased crack sensitivity.

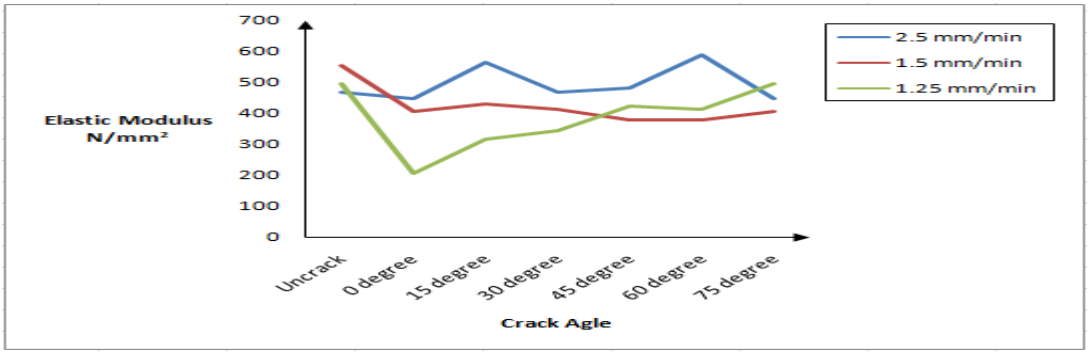

Fig: 4.3 Variation of elastic modulus with crack angle for different strain-rates

4.3 Variation of Ultimate Strength:

Ultimate strength represents the maximum stress that the material can withstand before failure. The ultimate strength values change according to both the crack angle and the loading rate, revealing trends that can help us understand how cracks affect gypsum's strength under different loading conditions.

A. Overview of Ultimate Strength Across Loading Rates

The Fig 4.4 includes three loading rates, each affecting the ultimate strength of rock samples with various crack angles, For 2.5 mm/min strain rate generally, higher ultimate strength values are observed at this loading rate across all angles. Faster loading rates often increase the material's apparent strength, as there is less time for cracks to propagate. For 1.5 mm/min strain rate the ultimate strength values are slightly lower than at 2.5 mm/min but still follow similar trends with respect to crack angles. For lower loading rate 1.15 mm/min lower ultimate strength values are observed, indicating that slower loading rates allow for more crack propagation and fracture development, reducing the overall strength.

B. Ultimate Strength for the Intact (Uncracked) Sample

The intact sample serves as a baseline for strength comparison across different crack angles. For each loading rate, the intact sample has the highest ultimate strength, showing the material's full capacity without any stress concentration points caused by cracks.

The ultimate strength decreases with the loading rate, with the highest value at 2.5 mm/min strain rate to 8.75 N/mm^2 and the lowest at 1.15 mm/min strain rate to 6.67 N/mm^2. This decrease is typical, as slower loading rates allow for more time-dependent failure mechanisms, such as crack growth.

C. Effect of Crack Angle on Ultimate Strength at Different Loading Rates

For 0° crack angle the ultimate strength is significantly lower than the intact sample, at 6.3 N/mm^2, showing that cracks aligned with the loading direction are particularly detrimental to strength. And for 15° to 30° crack angles the strength decreases further, reaching its lowest value

at 30° of 5.83 N/mm^2. These angles may allow cracks to propagate under the loading force, leading to greater material weakness. 45° crack angle shows there is a slight increase in ultimate strength at this angle 6.33 N/mm^2, indicating that cracks at a more oblique angle resist stress better than those closer to the loading direction. 60° and 75° crack angles shows the strength values increase, with 75° reaching a high value of 7.96 N/mm^2, close to the intact sample. This suggests that cracks at high angles have less impact on strength, as they do not open as readily under stress.

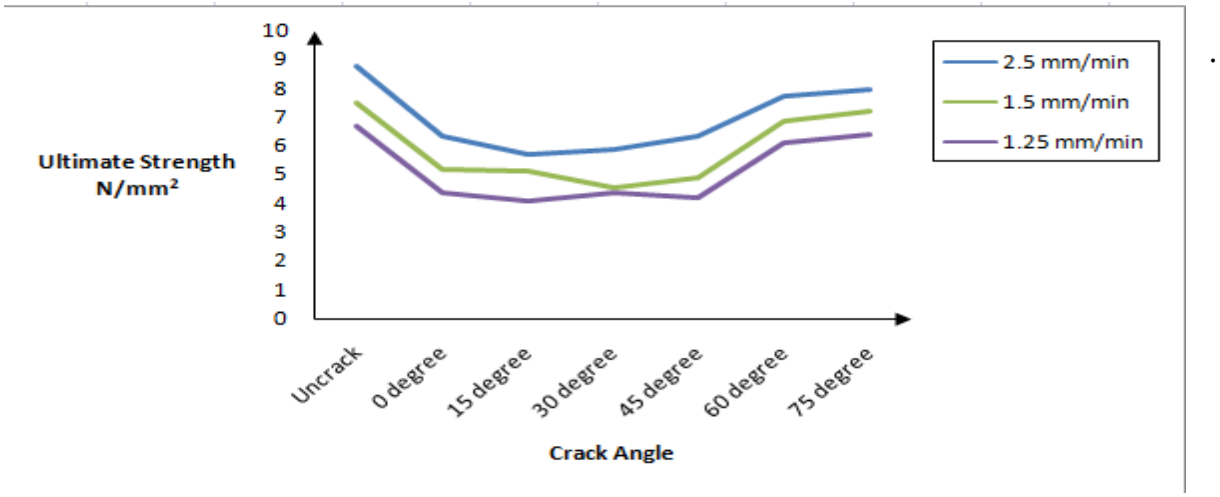

Fig 4.4 Variation of Ultimate strength with Crack Angle for different strain rates

4.4 Variation of Failure Strain:

The Fig shows the failure strain at different crack angles under three strain rates (2.5 mm/min, 1.5 mm/min, and 1.25 mm/min).

A. Observations by Crack Angle

For intact Specimen the failure strain is highest across all strain rates compared to cracked specimens. Values decrease as the strain rate decreases, 0.022 for 2.5 mm/min, 0.016 for 1.5 mm/min, and 0.016 for 1.25 mm/min. The failure strain at 0 degrees remains constant at 0.016 for both 2.5 mm/min and 1.5 mm/min but decreases to 0.012 at 1.25 mm/min. The failure strain for 15 degree decreases from 0.012 at 2.5 mm/min to 0.014 for both lower strain rates (1.5 mm/min and 1.25 mm/min).This indicates a minor increase in strain capacity with decreasing

strain rates at this angle. For 30 Degrees a slight decrease in failure strain from 0.016 at 2.5 mm/min to 0.014 at both 1.5 mm/min and 1.25 mm/min, suggesting a similar pattern to the 15-degree angle. For 45 Degrees similar to the 0-degree case, failure strain is consistent at 0.016 for 2.5 mm/min and 1.5 mm/min, then decreases slightly to 0.012 at 1.25 mm/min. For 60 Degrees Shows a unique trend where failure strain slightly increases from 0.016 at 2.5 mm/min to 0.022 at 1.5 mm/min and 0.024 at 1.25 mm/min. This trend suggests that at higher crack angles, lower strain rates improve failure strain. For 75 Degrees Failure strain is highest at 0.02 for 2.5 mm/min but decreases to 0.014 for both 1.5 mm/min and 1.25 mm/min, indicating a drop in failure strain as strain rate decreases.For lower crack angles, failure strain generally decreases with lower strain rates.At higher crack angles (particularly 60 degrees), the material shows increased failure strain at lower strain rates, possibly due to strain localization around cracks.The uncracked condition consistently shows the highest failure strain across all strain rates, which is expected as there is no pre-existing damage.

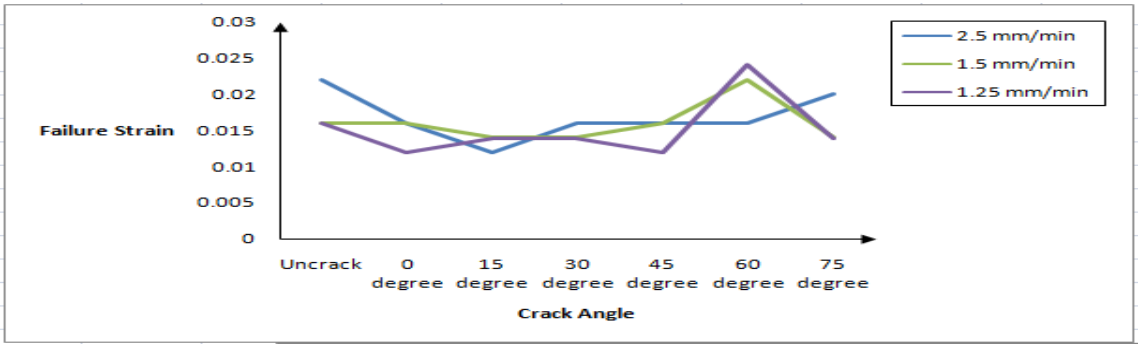

Fig 4.5 Variation of Failure strain with Crack angle for different strain-rates

4.5 Failure Pattern

A. Failure Initiation and Propagation in Intact (uncracked) Sample

The rock sample's failure initiation with higher strain rate of 2.5 mm/min Fig 4.6 (A) is more abrupt and concentrated near the center of the specimen. The material appears to have shattered and splintered, indicating brittle behavior. The failure propagates quickly, leading to sharp, distinct fragments. The radial cracks around the point of loading suggest that the material could not absorb or redistribute the energy efficiently, leading to immediate, widespread cracking and

fracture. This suggests that at a higher strain rate, the material undergoes rapid energy release, causing more severe damage. The sample failure initiation with 1.5 mm/min strain rate Fig 4.6 (B) is slightly more controlled, although cracks still appear centrally and propagate outwards. The cracks are less severe compared to the 2.5 mm/min sample, with some fragments remaining partially intact. This suggests that the material absorbs and dissipates some of the energy before complete failure occurs, leading to a less catastrophic propagation pattern. The relatively reduced strain rate allows the material to withstand a bit more stress, resulting in a less brittle failure than seen in the first image. The sample failure initiation with 1.25 mm/min strain rate fig 4.6(C) shows the least amount of fragmentation, failure initiation appears to be slower, with cracks forming gradually and propagating less aggressively. The rock sample maintains larger, coherent sections, which points to a more ductile response compared to the higher strain rates. The material has time to deform and distribute stresses over a larger area before complete failure, resulting in fewer, more stable cracks. This suggests that at lower strain rates, the material can accommodate more strain, delaying the onset of failure and resulting in less catastrophic crack propagation.

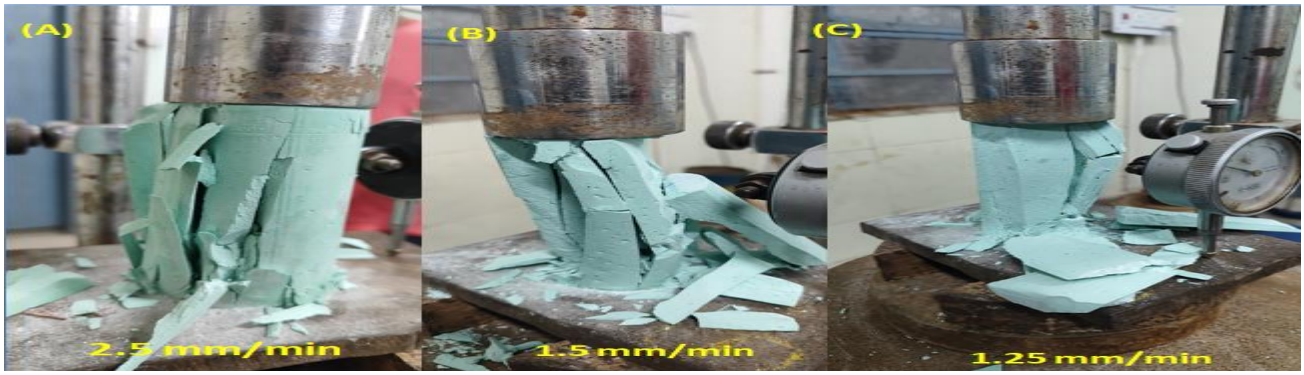

Fig:4.6. Failure pattern of uncrack sample for strain-rate (A) 2.5mm/min, (B)1.5mm/min and (C) 1.25mm/min

B. Failure Initiation and Propagation in 0˚ Sample

At higher strain rate of 2.5mm/min Fig 4.7 (A) shows the failure initiation is abrupt and concentrated near the center of the specimen. The sample exhibits significant fragmentation, with sharp, prominent cracks and splintering, indicating a brittle response. The cracks propagate

radially from the loading point, suggesting the material couldn't efficiently absorb or redistribute the applied energy, leading to rapid, widespread cracking and fracture. This behavior implies that at higher strain rates, the material undergoes rapid energy release, resulting in severe, brittle damage. At the moderate strain rate of 1.5 mm/min Fig 4.7 (B) shows the failure initiation is more controlled compared to the 2.5 mm/min rate, cracks still initiate centrally but propagate outward less aggressively. The cracks are less intense, with some fragments remaining partially intact, suggesting the material absorbed and dissipated some energy before complete failure. This strain rate appears to allow the material to withstand more stress, leading to a less catastrophic and slightly more controlled failure propagation. The reduced strain rate gives the material some ability to resist fracturing, resulting in a less brittle response than in the 2.5 mm/min strain rate case. And for the lower strain rate of 1.25 mm/min Fig 4.7 (C) shows the specimen exhibits minimal fragmentation. Failure initiation occurs slowly, with cracks forming gradually and propagating less aggressively. Larger the coherent sections of the specimen remain intact, indicating a more ductile-like behavior in comparison to the higher strain rates. The material appears to have had time to deform and distribute stresses more evenly before failing, leading to fewer, more stable cracks. This suggests that at lower strain rates, the material can accommodate more strain, delaying the onset of failure and reducing catastrophic crack propagation.

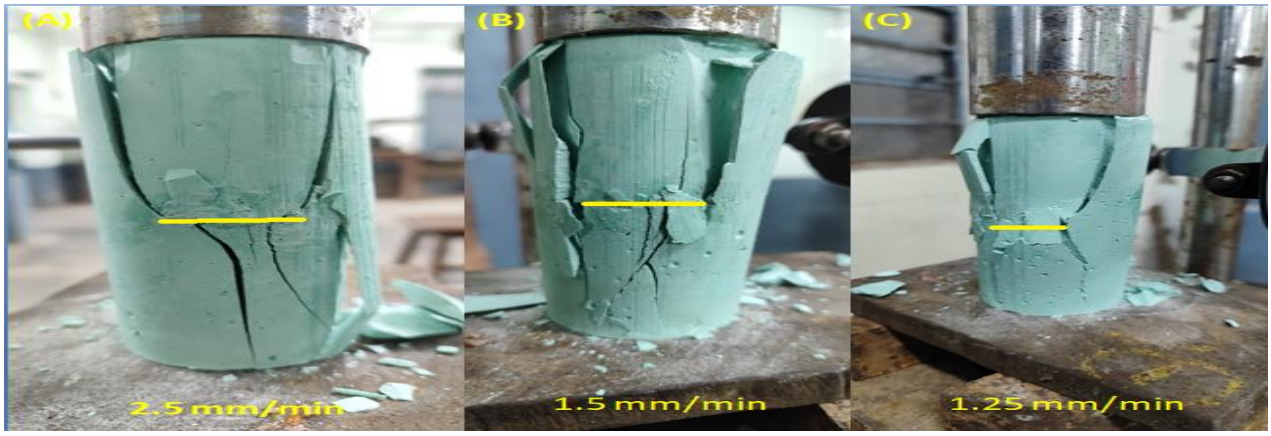

Fig:4.7 Failure pattern of 0˚ sample for strain-rate (A) 2.5mm/min, (B) 1.5mm/min and (C) 1.25mm/min

C. Failure Initiation and Propagation in 15˚ Sample

At higher strain rate of 2.5mm/min Fig 4.8 (A) shows the failure initiation appears abrupt, with prominent cracks developing near the center of the sample. The material shows extensive fragmentation and splintering, indicating a brittle response similar to the 0-degree samples. Radial cracks extend from the central loading area, suggesting that the material could not effectively absorb the energy, leading to rapid and widespread fracturing. This indicates that the higher strain rate causes a fast release of stored energy, resulting in intense, brittle failure. At the moderate strain rate of 1.5 mm/min Fig 4.8(B) shows the failure initiation is somewhat controlled, though cracks still form centrally and propagate outward. The cracks are less severe compared to the 2.5 mm/min rate, with some fragments remaining connected, suggesting partial energy absorption before complete failure. This reduced strain rate allows the material to dissipate stress to a degree, resulting in a less catastrophic failure than at 2.5 mm/min. The propagation is less violent, which points to a transition from a fully brittle response toward a slightly more ductile-like behavior. At the lower strain rate of 1.25 mm/min Fig 4.8 (C) shows the failure initiation is gradual, with less aggressive crack propagation and fewer fragments. The specimen maintains larger, cohesive sections, indicating a relatively more ductile behavior compared to the higher strain rates. The material appears to have had enough time to deform and distribute stress before failure, leading to fewer, more stable cracks. This suggests that the lower strain rate allows for a delayed failure onset, minimizing crack propagation and promoting larger, intact sections.

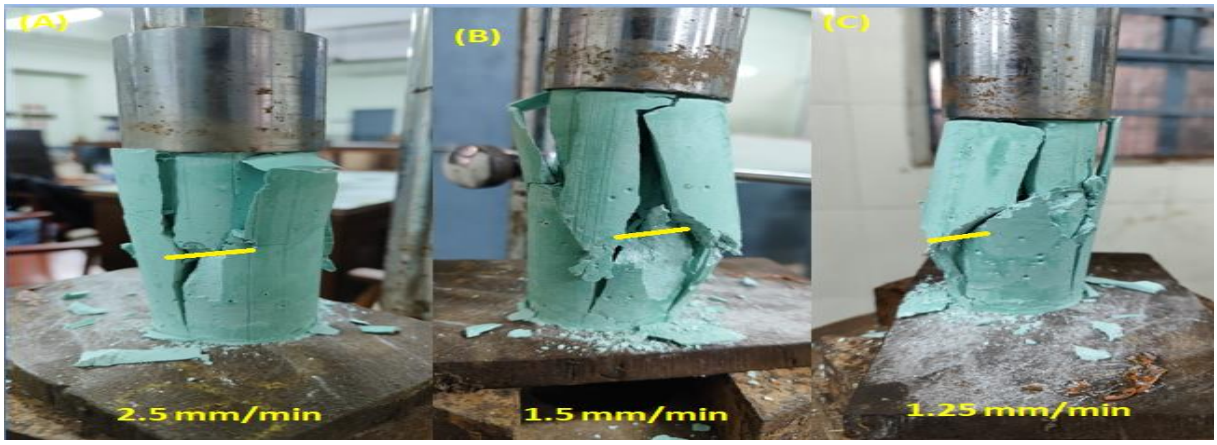

Fig:4.8 Failure pattern of 15˚ sample for strain-rate (A) 2.5mm/min, (B) 1.5mm/min and (C) 1.25mm/min

D. Failure Initiation and Propagation in 30˚ Sample

At the higher strain rate of 2.5mm/min Fig 4.9(A) shows the failure initiation is abrupt, with pronounced cracks and fragmentation throughout the sample. The specimen exhibits extensive shattering and large pieces breaking off, suggesting a brittle response to the applied load. Radial and angled cracks extend from the pre-existing crack, indicating that the material couldn't effectively redistribute the energy, leading to rapid, widespread fracturing. This suggests that the high strain rate causes an intense and brittle failure mode, with minimal energy dissipation. Lower strain rate of 1.5 mm/min Fig 4.9(B) shows the failure initiation is more gradual compared to the 2.5 mm/min sample. Cracks initiate from the central area but propagate outward in a more controlled fashion. The cracks are less severe than in the 2.5 mm/min case, with larger fragments staying partially intact, implying that some of the applied energy is absorbed before full failure occurs. The reduced strain rate results in a slightly less violent propagation, suggesting a shift toward a less brittle, slightly more ductile-like response. At 1.25 mm/min strain rate Fig 4.9(C) depicts the failure initiation appears to be more controlled, with cracks forming and propagating gradually. The material appears to have had enough time to redistribute stresses before fracturing completely, leading to a more stable crack pattern and fewer fragments. This implies that the lowest strain rate enables the material to resist failure longer and absorb more energy, resulting in less catastrophic propagation.

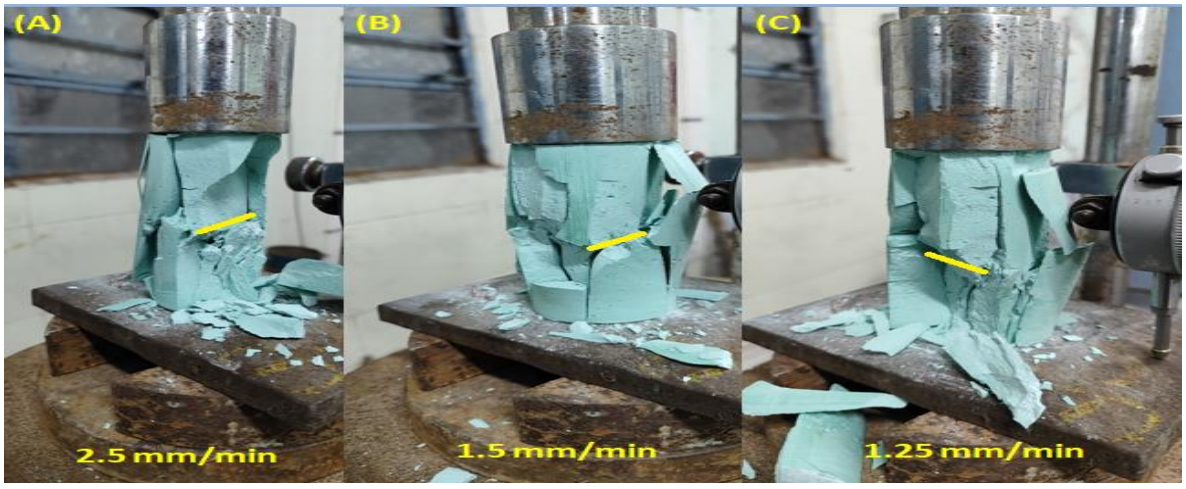

Fig:4.9 Failure pattern of 30˚ sample for strain-rate (A) 2.5mm/min, (B)1.5mm/min and (C)1.25mm/min

E. Failure Initiation and Propagation in 45˚ Sample

At higher strain rate of 2.5mm/min Fig 4.10 (A) depicts the failure initiation in this image is characterized by an abrupt, significant crack near the pre-existing 45-degree angle. The central area shows a high level of fragmentation, indicating a sudden and brittle response of the gypsum under this strain rate. The cracks propagate quickly and extensively, leading to sharp and fragmented pieces. The rapid spread of cracks shows that the material cannot distribute the applied load evenly, resulting in a brittle, splintered failure pattern. The higher strain rate of 2.5 mm/min causes a quick energy release, leading to catastrophic failure with multiple, severe radial cracks. At the 1.5 mm/min strain rate Fig 4.10 (B) shows the failure initiation at this strain rate shows more controlled crack formation compared to the 2.5 mm/min sample. The initial cracks still appear near the 45-degree plane, but they spread less aggressively. The crack propagation in this sample is less severe, resulting in some fragments remaining partially attached. This indicates that the material is better able to absorb and dissipate energy before complete failure, leading to a less brittle propagation pattern. The 1.5 mm/min strain rate demonstrates a moderate failure response where the material can resist some of the load without immediate catastrophic failure. At the lower strain rate of 1.25 mm/min Fig 4.10 (C) shows the initiation of failure at this lower strain rate appears more gradual. The formation of cracks starts more slowly, with less initial fragmentation. The cracks propagate in a more controlled manner, maintaining larger sections of intact material. The 1.25 mm/min strain rate results in the most stable failure, showing larger, cohesive pieces after cracking. The rock sample accommodates more strain and delays failure, leading to a less catastrophic outcome.

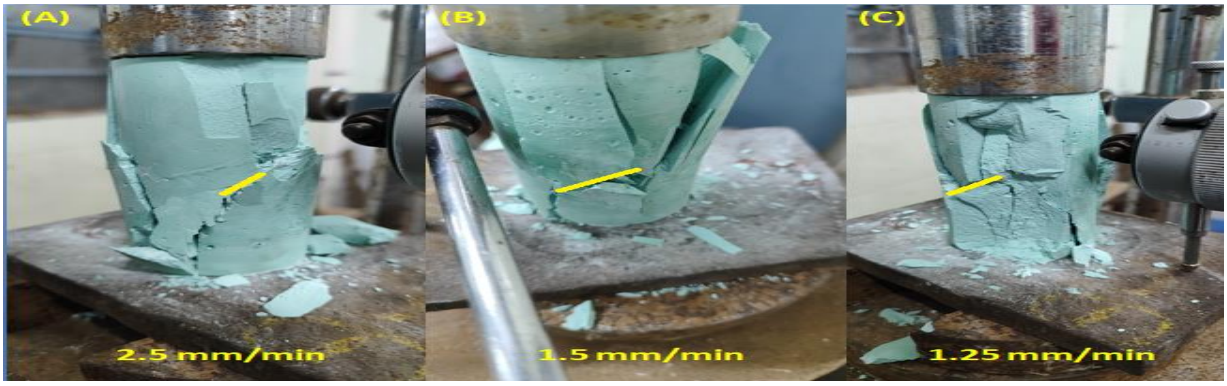

Fig:4.10. Failure pattern of 45˚ sample for strain-rate (A) 2.5mm/min, (B)1.5mm/min and (C) 1.25mm/min

F. Failure Initiation and Propagation in 60˚ Sample

At higher strain rate of 2.5 mm/min Fig 4.11 (A) shows the failure initiation of failure at the highest strain rate of 2.5 mm/min is marked by a rapid and sudden development of major cracks. These cracks start from the central region and extend outwards, indicating a brittle response. The crack propagation is aggressive and extensive, leading to a large number of small, sharp fragments. The high strain rate leads to an inability of the rock sample material to redistribute the applied load evenly, resulting in a catastrophic and splintered failure pattern. At the moderate strain rate 1.5 mm/min Fig 4.11 (B) shows the initiation of cracks is more controlled compared to the 2.5 mm/min sample. The initial cracks appear near the 60-degree orientation but spread in a slightly more contained manner. The cracks propagate with moderate severity, leading to some sections of the material remaining attached even after the main failure occurs. This indicates that the material at this rate is capable of absorbing and redistributing energy better than at the higher strain rate. The 1.5 mm/min strain rate shows an intermediate failure behavior, where the response is less brittle than the 2.5 mm/min strain rate but not as ductile as lower rates. The material exhibits partial fragmentation with sections of cohesive material present after failure. At the lower strain rate of 1.25 mm/min Fig 4.11 (C) revel the failure initiation occurs more gradually compared to the higher strain rates. Initial cracks appear with less fragmentation and develop over time. The propagation of cracks at this lower strain rate is more stable, with larger intact pieces remaining after failure. The 1.25 mm/min strain rate results in a more controlled and stable failure, producing fewer fragmented pieces and larger cohesive sections. The response indicates that the gypsum can accommodate more strain before failure.

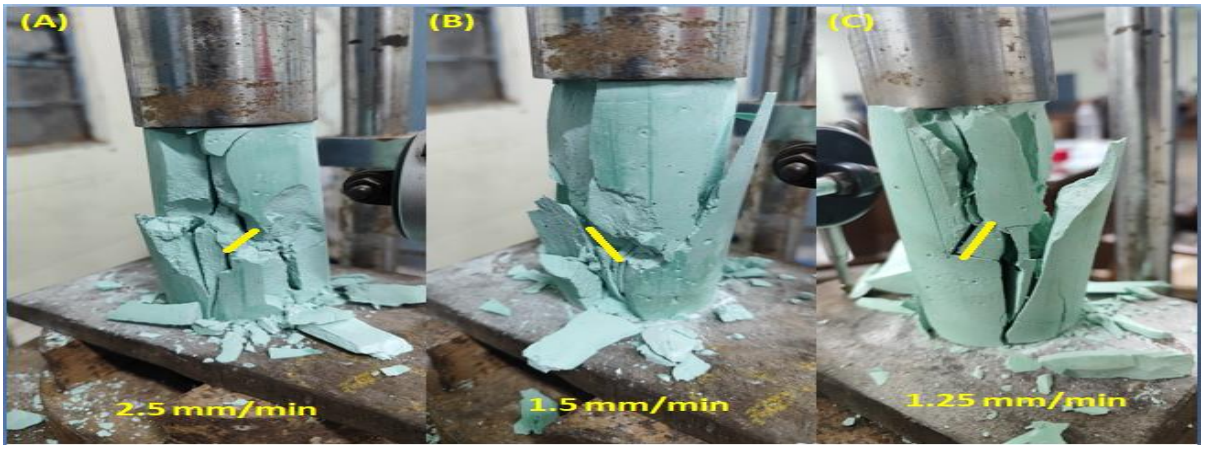

Fig:4.11 Failure pattern of 60˚ sample for strain-rate (A) 2.5mm/min, (B)1.5mm/min and (C) 1.25mm/min

G. Failure Initiation and Propagation in 75˚ Sample

At the higher strain rate of 2.5mm/min Fig 4.12 (A) shows the failure initiation is characterized by the sudden appearance of significant vertical cracks near the 75-degree orientation. The initiation is abrupt, indicating a brittle response of the gypsum material. The cracks propagate rapidly, leading to fragmentation and splitting of the sample into several large and sharp sections. The 2.5 mm/min strain rate results in a brittle and catastrophic failure pattern, with extensive vertical cracking and considerable fragmentation. At the moderate strain rate of 1.5 mm/min Fig 4.12 (B) shows the failure initiation is more gradual compared to the 2.5 mm/min rate. Cracks still begin near the 75-degree orientation, but the initial formation is less aggressive. The crack propagation at this strain rate is less severe, resulting in cracks that develop without complete detachment of material. Some portions of the sample remain intact, indicating the material's ability to absorb and manage some of the applied stress before failure. The 1.5 mm/min strain rate demonstrates an intermediate response between brittle and ductile behavior. The cracks are pronounced but do not propagate as violently as in the higher strain rate. At the lower strain rate of 1.25 mm/min Fig 4.12 (C) revel the initiation of failure is more controlled and starts with smaller cracks. These cracks take more time to form and show a less abrupt initiation. Crack propagation is stable, maintaining larger sections of the sample even as cracks spread. The propagation pattern suggests a more ductile-like response, where the material can better handle stress redistribution before complete failure occurs. The 1.25 mm/min strain rate results in the most stable failure pattern. The cracks develop gradually, leading to a less fragmented structure and larger cohesive pieces remaining intact after failure.

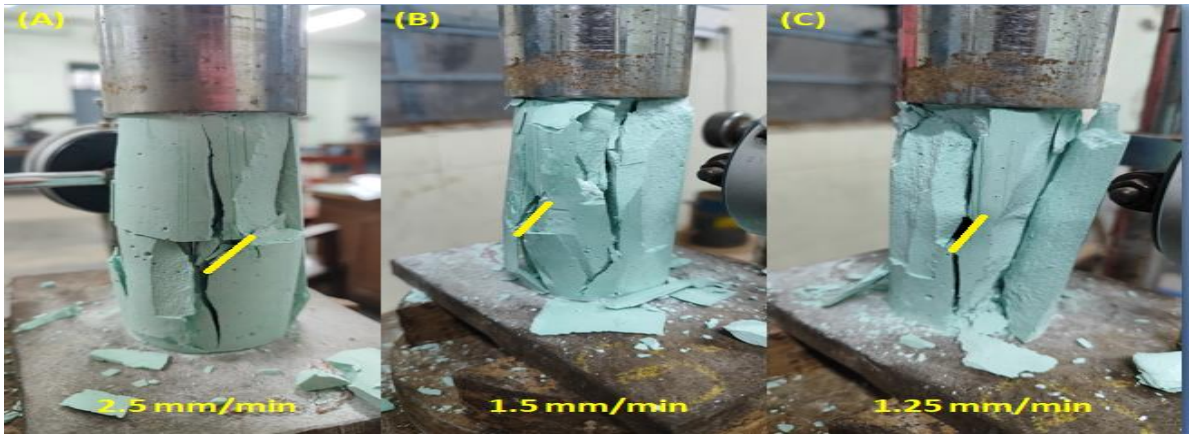

Fig:4.12 Failure pattern of 75˚ sample for strain-rate (a) 2.5mm/min, (b) 1.5mm/min and (c)1.25mm/min

Chapter 5

CONCLUSION

This study aims to highlights the importance of displacement rates and joint orientation in influencing the mechanical behavior of soft rock analogs. Key findings include:

I. Strain Rate and Strength**:** Higher displacement rates led to increased strength in both intact and jointed samples, with a noticeable improvement up to a critical rate. Samples with joint orientations closer to the loading direction demonstrated higher strength, indicating a rate-dependent response in material performance.

II. Elastic Modulus Variability**:** Stiffness varied with both strain rate and joint orientation. Higher strain rates increased the elastic modulus, while certain orientations (e.g., 0° and 45°) reduced stiffness more significantly, highlighting the susceptibility of these orientations to early deformation.

III. Failure Patterns**:** The failure mode shifted from brittle at higher strain rates to ductile at lower rates. Samples with higher joint orientations (60° and 75°) showed a prominent transition from brittle to ductile behavior as displacement rates decreased, indicating a greater capacity for energy absorption before failure.

IV. Fracture Mechanisms**:** A transition from tensile to shear fractures was observed at higher strain rates, especially in samples with a greater persistence ratio. This shift underlines the complex fracturing mechanisms that occur under varied loading conditions.

These findings the need for considering both strain rate and joint orientation in engineering contexts such as mining and slope stability where dynamic loading is a factor. Future research could extend to a wider range of strain rates and different rock-like materials to deepen understanding of these behaviors under diverse conditions

Reference

1. Reik, G., & Zacas, M. (1978, December). Strength and deformation characteristics of jointed media in true triaxial compression. In *International Journal of Rock Mechanics and Mining Sciences & Geomechanics Abstracts* (Vol. 15, No. 6, pp. 295-303). Pergamon.

2. Bésuelle, P., Desrues, J., & Raynaud, S. (2000). Experimental characterisation of the localisation phenomenon inside a Vosges sandstone in a triaxial cell. *International Journal of Rock Mechanics and Mining Sciences*, *37*(8), 1223-1237.

3. Sun, S., Sun, H., Wang, Y., Wei, J., Liu, J., & Kanungo, D. P. (2014). Effect of the combination characteristics of rock structural plane on the stability of a rock-mass slope. *Bulletin of Engineering Geology and the Environment*, *73*, 987-995.

4. Alejano, L. R., Arzúa, J., Bozorgzadeh, N., & Harrison, J. P. (2017). Triaxial strength and deformability of intact and increasingly jointed granite samples. *International Journal of Rock Mechanics and Mining Sciences*, *95*, 87-103.

5. Roshan, H., Masoumi, H., & Regenauer-Lieb, K. (2017). Frictional behaviour of sandstone: a sample-size dependent triaxial investigation. *Journal of Structural Geology*, *94*, 154-165.

6. Wei, S., Wang, C., Yang, Y., & Wang, M. (2020). Physical and mechanical properties of gypsum-like rock materials. *Advances in Civil Engineering*, *2020*, 1-17.

7. Mathur, G. K., Maji, V., Misra, S., & Tiwari, G. (2022). Effect of displacement rates on the mechanical integrity of soft-porous rock analogue containing non-persistent joints of variable lengths. *Journal of Earth System Science*, *131*(2), 118.

8. González-Fernández, M. A., Estévez-Ventosa, X., Alejano, L. R., & Masoumi, H. (2023). Size-dependent behaviour of hard rock under triaxial loading. *Rock Mechanics and Rock Engineering*, 1-17.

9. Smith, J. D., & Collins, R. L. (2002). Influence of joint spacing and orientation on rock slope stability. Journal of Geotechnical and Geoenvironmental Engineering, 128(7), 573-582.
10. Lee, M., & Moon, W. (2004). Shear behavior of jointed rock masses under dynamic loading conditions. Rock Mechanics and Rock Engineering, 37(3), 153-165.
11. Liu, Q., Wang, X., & Wang, J. (2006). Effect of water saturation on the mechanical properties of sandstone. Engineering Geology, 85(1-2), 180-192.
12. Huang, Z., & Yang, Z. (2008). Numerical modeling of jointed rock masses in uniaxial compression. Computers and Geotechnics, 35(4), 561-569.
13. Li, H., & Gao, Y. (2011). Strength degradation and failure patterns in limestone under cyclic loading. International Journal of Rock Mechanics and Mining Sciences, 48(6), 1016-1024.
14. Chen, H., Li, X., & Tang, C. (2015). Crack propagation and coalescence in rock materials with two non-persistent joints under uniaxial loading. Rock Mechanics and Rock Engineering, 48(4), 1569-1581.
15. Zhang, J., & Xu, L. (2016). Anisotropic mechanical behavior of shale: Effects of bedding orientation on strength and deformability. Journal of Petroleum Science and Engineering, 138, 169-178.
16. Wang, R., & Zhao, Y. (2017). Influence of joint roughness and stress conditions on rock shear strength. Geomechanics and Geophysics for Geo-Energy and Geo-Resources, 3(2), 129-137.
17. Kim, S., & Park, J. (2018). Size effect on uniaxial compressive strength and failure behavior of granite samples. International Journal of Rock Mechanics and Mining Sciences, 103, 50-57.
18. Bai, Q., & Huang, Q. (2019). Investigating the deformation behavior of fractured rock masses under confining pressure. Journal of Rock Mechanics and Geotechnical Engineering, 11(3), 595-603.